

# Study of Flow and Heat Transfer in High Pressure Die Casting Cooling Channel



K. ARUNKUMAR, SHAMIT BAKSHI, GANDHAM PHANIKUMAR,  
and T.V.L. NARASIMHA RAO

High-pressure die casting (HPDC) is a widely used process with short cycle times to manufacture complex shapes of aluminium castings for the automotive industry. Most of the die casting companies use specialized commercial software to simulate molten metal filling and solidification. This approach works satisfactorily and is industrially accepted for defect prediction capability. Die cooling is an effective technique to reduce internal porosity in die cast components. But die cooling process is not completely captured in the approach used in the casting simulations. This often resulted in false positives in the defect predictions. One of the main reasons for the lack of precision in simulation is the uncertainty in assigning the boundary conditions such as heat transfer coefficients (HTC) for the die cooling channel. In this study, a coupled simulation strategy was developed to determine accurate HTC values of the die cooling channel. The computational domain was divided into two sub-domains, *i.e.*, casting zone and die cooling zone. Two different industrially accepted simulation tools were used: (a) for casting simulation and (b) for turbulent fluid flow and heat transfer simulation in the cooling channel. A series of iterations were performed by exchanging information at the interface between the two sub-domains till the convergence was achieved. Experiments were also conducted with a thermocouple inserted in the die and the actual die temperature readings were measured. The converged simulation results agreed well with the experimental measurements. Also, the influence of flow rate on HTC was studied by conducting experiments with two different flow rates and the castings produced were analyzed with the help of CT scan analysis, micro-structure evaluation and thermal imaging. The obtained results demonstrated the efficacy of the method adopted in prescribing the values of heat transfer conditions in casting simulations. With the coupled simulation approach developed in this work, parametric studies were conducted to maximize the heat removal rate from a given die, for different flow velocities, nozzle diameters, cooling hole diameters and nozzle-to-surface spacings.

<https://doi.org/10.1007/s11663-023-02785-6>

© The Minerals, Metals & Materials Society and ASM International 2023

## I. INTRODUCTION

HIGH-PRESSURE die casting (HPDC) is a widely used process with short cycle times of processing to manufacture complex shapes of aluminium castings for the automotive industry. As a part of die casting design,

simulation plays a major role in predicting the defects and taking the corrective actions to prevent these defects. There are several casting simulation softwares available in the market and a representative list is provided in the Table I.<sup>[1]</sup> Among these, most of the die casting companies use specialized commercial software to simulate molten metal filling and solidification. This approach works satisfactorily and is industrially accepted for defect prediction capability.

In die casting, die cooling is an effective technique to increase productivity and reduce internal porosity. By introducing a cooling channel in a core pin, the porosity can be shifted away from its surface and intensity of porosity can be reduced significantly. This actual behaviour of casting on account of die cooling is not completely captured in the standard approach used in the casting simulation. One of the main reasons for the lack of precision in simulation is the uncertainty in assigning the boundary condition for heat transfer

---

K. ARUNKUMAR is with the R&D, Sundaram Clayton Limited, Padi, Chennai 600050, India. Contact e-mail: karunmechanizer@gmail.com and also with the Department of Mechanical Engineering, IIT Madras, Chennai, 600036, India. SHAMIT BAKSHI is with the Department of Mechanical Engineering, IIT Madras. GANDHAM PHANIKUMAR is with the Department of Metallurgical and Materials Engineering, IIT Madras, Chennai, 600036, India. T.V.L. NARASIMHA RAO is with the R&D, Sundaram Clayton Limited.

Manuscript submitted November 9, 2022; accepted March 17, 2023.  
Article published online April 26, 2023.

**Table I. Representative List of Casting Simulation Software Tools<sup>[1]</sup>**

S. No.	Software	Solution Feature
1	MAGMASOFT <sup>®</sup>	FDM
2	Flow-3D <sup>®</sup>	VOF
3	ADSTEFAN <sup>®</sup>	FDM
4	Procast <sup>®</sup>	FEM
5	NovaFlow <sup>®</sup>	FDM
6	Cast CAE <sup>®</sup>	FVM
7	Wincast <sup>®</sup>	FEM
8	AnyCasting <sup>®</sup>	FDM
9	Autocast <sup>®</sup>	GVM
10	Solid cast <sup>®</sup>	FDM

The abbreviations used are as follows: Finite Difference Method (FDM), Volume of Fluid Method (VOF), Finite Element Method (FEM) and Gradient Vector Method (GVM).

coefficient for the die cooling channel.<sup>[2]</sup> The commercial software tools, although good at simulating molten metal filling and solidification, lack features for a sufficiently detailed prescription of heat transfer coefficients as boundary conditions. Generally, averaged heat transfer coefficient (HTC) values are prescribed and recommended as the boundary conditions (Figure 1). This often leads to false positives in prediction of casting defects—particularly the presence of undesirable inter-metallic compounds that can be identified during the X-ray radiography of the cast component. A strong correlation between the defect prediction by the casting simulation and the defect characterization by the non-destructive evaluation is important to achieve higher productivity.

In an earlier work, this uncertainty of the boundary condition in the cooling channel was quantified and the effect was studied in terms of casting quality and design of casting process.<sup>[2]</sup> In another work, a numerical model was used to predict the heat transfer behaviour in die casting cooling channel.<sup>[3]</sup> The results were compared with Gnielinski heat transfer empirical relation and a good agreement was observed in the straight portion of cooling channel (see Figure 1) whereas the equation failed to predict the heat transfer at the tip portion of cooling channel. Similar to this, a numerical investigation was performed to study the turbulent flow and heat transfer of liquid nitrogen ( $LN_2$ ) within a cryoprobe.<sup>[4]</sup> These studies inferred that the convective heat transfer at tip zone was much higher than the heat transfer at straight portion of cooling channel. The geometry of cooling channel and Reynolds number had a significant impact on heat transfer.

Because of a lack of accuracy in the HTC values, the simulations fails to capture certain undesirable effects in actual casting process such as inadequate cooling, excessive cooling and improper thermal management of dies. This further leads to casting defects such as lamination, cold shut, non fill, flow porosity, shrinkage porosity, soldering, drag, crack and heat check marks. In addition, the designer is led to consider other options

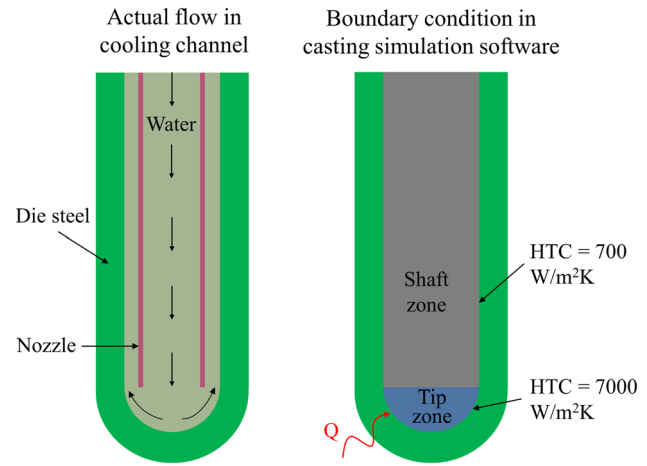


Fig. 1—Schematic of the cooling channel as an insertion in the die casting setup. Water flow through the cooling channel is not considered in the casting simulation. Some recommended and averaged HTC values of 7000 and 700 W/m<sup>2</sup>K are given as boundary condition at tip and shaft zones in cooling channel respectively.

instead of an accurate cooling channel. Such iterations to arrive at reduced defect in the cast component could involve loss in productivity.

Open literature on the modeling of the cooling channel in a die casting setup is scarce and there was no attempt to determine accurate HTC values. Also, experimental validation of the simulation was not available. In the advent of Gigacasting for large automotive components in the electrical vehicle industry, these studies are critical to develop novel Al-based alloy components for lightweighting.

The objective of this study is to develop a methodology to determine accurate heat transfer coefficient values on the cooling channel surface and use it for the casting simulation. The results are also validated with experimental data. Various parameters influencing the cooling such as flow velocity, nozzle diameter, cooling hole diameter and nozzle-to-surface spacing are varied to maximize the heat removal rate by the cooling medium.

## II. METHODOLOGY

### A. Selection of Casting and Cooling Geometry

In pressure die casting process, normally a cooling circuit will be enabled during solidification phase. So, it is appropriate that HTC of cooling channel has to be evaluated in this phase. The casting geometry was selected in such a way that it should have near-axisymmetric features, cooling provision and ease of incorporation of a thermocouple in it (Figure 2). A cooling hole diameter of 10 mm was taken for analysis as it is predominantly used in HPDC dies as a local industrial practice.

## B. Coupled Simulation Strategy

The entire domain of interest is divided into two sub-domains and different numerical methods are used in these domains separately. The two sub-domains are coupled by exchanging their solutions at the interface. The purpose of this coupling is to gain the advantages of appropriate numerical tool in each domain and thus to improve the accuracy of the simulation. This approach is referred to as ‘‘coupled modeling approach’’.[5] The coupled modeling approach is continued till the calculated cooling rates are converged. Cooling rate plays an important role in the formation of intermetallic compounds during solidification of Al-alloys typically used in the HPDC industry.

In this study, the computational domain was divided into two sub-domains namely, casting zone and die cooling zone. Casting simulation was performed using MAGMASOFT® (FDM), a tool that has industrially accepted prediction capability for casting defects. Similarly cooling channel simulation should involve the ability to model the complex turbulent flow with heat transfer accurately. ANSYS Fluent® (FVM) was used in the die cooling zone for turbulent fluid flow and heat transfer. Figure 3 shows the schematic of the domains used for this coupled modeling approach.

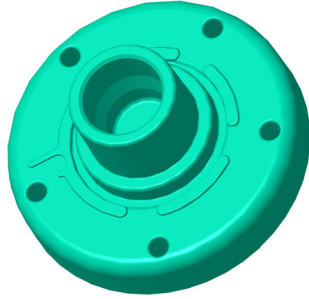


Fig. 2—A casting geometry with simple shape, near-axi-symmetric features and ease of adoption of a thermocouple selected for analysis.

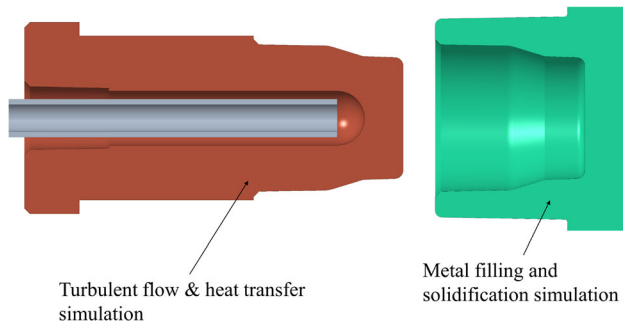


Fig. 3—Schematic showing the domains used for turbulent fluid flow and heat transfer simulation (left) and aluminium casting simulation (right).

## C. Modeling of Cooling Channel Simulation

### 1. Selection of turbulence model

At any location within the cooling nozzle, the Reynolds number was observed to be close to 10,000. So, the flow in the cooling channel can be considered turbulent.[6] There were many studies available to model the turbulent flow of jets impinging on concave surfaces. Based on the literature survey,[3,4,6-11] realizable  $k-\epsilon$  model with enhanced wall treatment was selected for analysis because it showed least deviation from experimental values. Based on the recommendations from literature, a  $y^+$  value of less than 1 was ensured for near wall treatment to capture the viscous sub layer effectively.

The domain of interest was divided into multiple cells in ANSYS meshing tool as shown in Figure 4. Mesh refinement study was carried out from the element size of 0.12 to 0.06 mm in steps of 0.02 mm. The heat transfer coefficient results did not change significantly for the 0.06 and 0.08 mm element sizes. Therefore element size of 0.08 mm was used for numerical simulation and the domain was discretized into 1,53,056 cells.

### 2. Governing equations

The realizable  $k-\epsilon$  model uses alternative formulation and modified transport equation for turbulent viscosity and dissipation rate, respectively. The governing equations are as follows[4,12]:

Continuity equation:

$$\nabla(\rho\bar{\mathbf{U}}) = \mathbf{0} \quad [1]$$

Momentum and turbulence transport equations:

$$\frac{D(\rho\bar{\mathbf{U}})}{Dt} = -\nabla(\mathbf{p}) + \mu_{\text{eff}} \cdot \nabla^2(\rho\bar{\mathbf{U}}) \quad [2]$$

$$\frac{\partial(\rho\kappa)}{\partial t} + \nabla(\rho\kappa\bar{\mathbf{U}}) = \nabla[(\mu + \frac{\mu_t}{\sigma_\kappa}) \cdot \nabla\kappa] + \mathbf{G}_\kappa - \rho\epsilon \quad [3]$$

$$\frac{\partial(\rho\epsilon)}{\partial t} + \nabla(\rho\epsilon\bar{\mathbf{U}}) = \nabla[(\mu + \frac{\mu_t}{\sigma_\epsilon}) \cdot \nabla\epsilon] - \rho C_2 \frac{\epsilon^2}{\kappa + \sqrt{\epsilon\nu}} \quad [4]$$

Energy equation

$$\rho C_p \frac{DT}{Dt} = \nabla(k_{\text{eff}}\nabla T) \quad [5]$$

where  $\rho$  is the density of water,  $\bar{\mathbf{U}}$  is the velocity vector,  $k$  is the thermal conductivity of water,  $C_p$  is the specific heat of water,  $\kappa$  is the turbulent kinetic energy,  $p$  is pressure,  $\epsilon$  is the turbulence dissipation rate,  $\mu_{\text{eff}}$  is the effective viscosity ( $\mu_{\text{eff}} = \mu + \mu_t$ ),  $\mu$  is the molecular viscosity,  $\mu_t$  is the eddy viscosity,  $\mu_t = \rho C_\mu \kappa^2 / \epsilon$ ,  $G_\kappa$  is the generation of turbulent kinetic energy,  $T$  is the temperature,  $k_{\text{eff}}$  is the effective thermal conductivity,  $\sigma_\kappa$ ,  $\sigma_\epsilon$  and  $C_2$  are the model constants (1.0, 1.2 and 1.9 respectively). Expressions modeling  $G_\kappa$ ,  $C_\mu$  and  $k_{\text{eff}}$  can be found in Fluent user manual.[12]

### 3. Boundary conditions

Since the analysis involved conduction with forced convection, coupled heat transfer was assigned at the solid–liquid interface. The analysis was conducted for an unsteady, axi-symmetric, flow with constant fluid properties. The effect of radiative heat transfer and gravity were ignored.

Figure 5 illustrates the boundary conditions assigned in the turbulent flow modeling. H13 steel was used for solid core pin. Water was used as the fluid medium in the cooling channel. The contour which was in contact with the casting was split into 5 different curves as shown in Figure 5. There were 72 virtual thermocouple points placed equally on these curves in casting simulation. So each curve had a set of different points based on its length. Temperature values were taken at these thermocouple points for the solidification time of 15 s. Using these temperature profiles, an empirical equation was fit for each curve using a MATLAB® script to determine the temperature as a function of time and positions (Figure 6).

The temperature function of any curve is represented in Eq. [6] which is the polynomial function of order 5 in time and of order 1 in positions. The polynomial coefficients are different for each curve. These temperature functions were given as input boundary condition to cooling channel simulation.

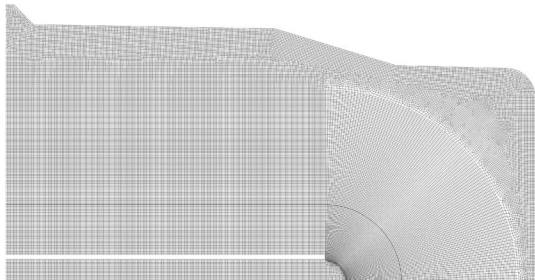


Fig. 4—Unstructured mesh distribution with quadrilateral shape element is used in the computational domain.

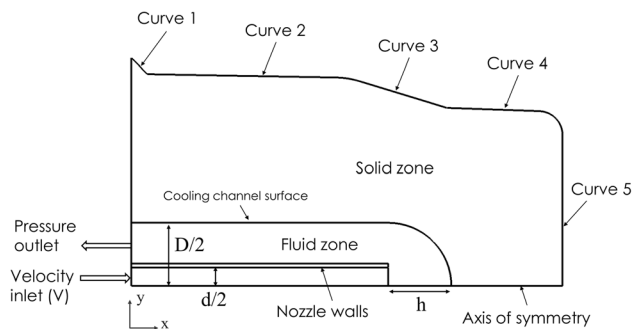


Fig. 5—Boundary conditions in the turbulent flow modeling.

$$T = a_0 + a_1(x + y) + a_2t + a_3(x + y)t + a_4t^2 + a_5(x + y)t^2 + a_6t^3 + a_7(x + y)t^3 + a_8t^4 + a_9(x + y)t^4 + a_{10}t^5 \quad [6]$$

SIMPLE algorithm was used for pressure–velocity coupling. For discretization of momentum and energy equations, second order upwind scheme was used. The simulation was said to be converged if a residual value of  $10^{-5}$  was attained.

### D. Modeling of Casting Simulation

The complex geometry was discretized into 3,64,695 cells using cuboid element of 0.8 mm (Figure 7) in a standard meshing procedure explained in the manual.<sup>[13]</sup> The solidification calculation is performed using the energy equation.<sup>[2,13,14]</sup>

$$\rho_m C_{pm} \frac{\partial T}{\partial t} = \lambda \nabla^2 T + \dot{Q}''' \quad [7]$$

where  $\rho_m$ ,  $C_{pm}$  and  $\lambda$  are density, specific heat and thermal conductivity of metal, respectively.  $\dot{Q}'''$  is heat source term and this accounts for latent heat during the phase change.

$$\dot{Q}''' = \begin{cases} 0, & \text{for } T > T_L \\ \frac{\partial f_s}{\partial T} \frac{\partial T}{\partial t} \rho L, & \text{for } T_S < T < T_L \\ 0, & \text{for } T < T_S, \end{cases} \quad [8]$$

where  $f_s$  is solid fraction and this is a temperature dependant material property based on experimental measurements,  $L$  is latent heat,  $T_S$  is solidus temperature and  $T_L$  is liquidus temperature. HTC at the channel wall was used as the boundary condition in this casting simulation. The HTC values were obtained from the cooling channel simulation.

### E. Simulation Procedure

1. With the generally recommended HTC values as an initial guess, a casting simulation was performed for

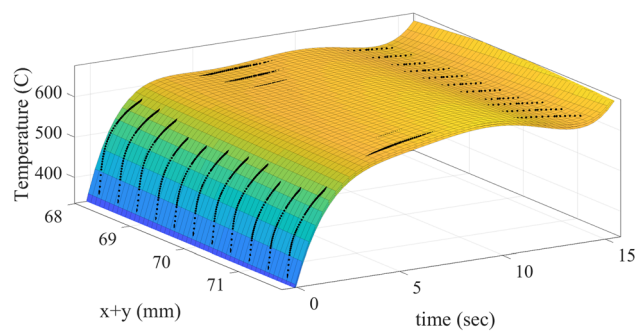


Fig. 6—A polynomial surface is fitted using MATLAB script for curve 3 which has eleven points. The goodness of fit is ensured by tracking its  $R^2$  value (99.8 pct).



the casting zone. This is marked as 'Input to casting simulation (1)' in Figure 8.

- The temperature values at the interface as calculated from the above simulation was transformed into the empirical equation. These temperatures as functions were given as input boundary condition for cooling channel simulation (Figure 6 and Eq. [6]). Cooling channel simulation was performed in die cooling zone.
- The HTC values were taken as output from the above cooling channel simulation. This is marked as 'Output from cooling channel simulation (1)' in Figure 8. The continuous function was converted to a piecewise step function marked as 'Input to casting simulation (2)'. Using the revised HTC values, another casting simulation was carried out.
- Using the new temperature values, cooling channel simulation was repeated (same as step 2).
- All the above steps were repeated till the difference of HTC values between the current iteration and previous iteration are within a residual of  $10^{-5}$ .

This series of iterations was executed since the initial HTC values were incorrect which could lead to wrong temperature values. Using this coupled simulation strategy, the results are expected to adjust to increase the simulation accuracy.

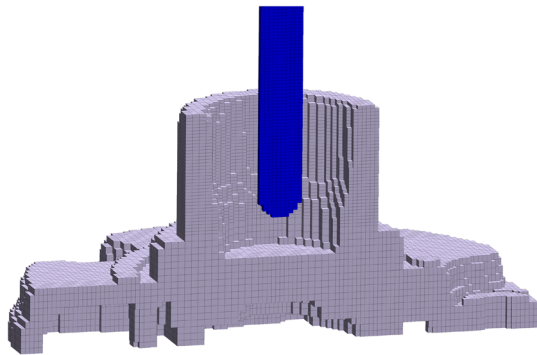


Fig. 7—Adaptive meshing in casting simulation software.

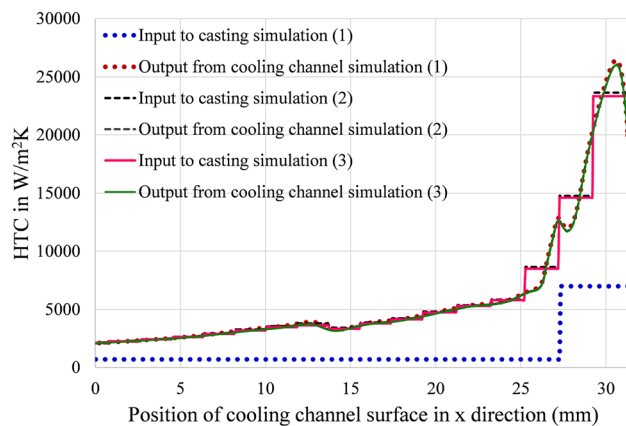


Fig. 8—Plots of HTC on the cooling channel surface with x for coupled modeling approach.

### 1. Simulation results

HTC of  $7000 \text{ W/m}^2\text{K}$  and  $700 \text{ W/m}^2\text{K}$  were the initial guess as per recommended values at the impingement zone and straight zone of the cooling channel respectively. Coupled modeling approach was performed using the steps mentioned in the simulation procedure. HTC values at different stages of the calculation are plotted in the graph as shown in Figure 8. There is a significant difference in HTC between the initial guess (maximum HTC =  $7000 \text{ W/m}^2\text{K}$ ) and the output from cooling channel simulation (3) (maximum HTC =  $26,000 \text{ W/m}^2\text{K}$ ). The reason is that the water flow and heat transfer are studied in turbulent flow simulations separately and merged with casting simulation using the coupled modeling approach (Figure 8).

The effect of flow rate on HTC was studied numerically by changing the flow rate values from 1 to 5 L/min. The complete procedure of coupled modeling simulation was repeated for 5 L/min. The HTC values are plotted in Figure 9 for both flow rates. Similar qualitative variation of HTC values is observed in 5 L/min simulation. Though the pattern looks same for both the flow rates, there is a drastic increase in HTC values especially at positions near the tip of the cooling channel. The maximum value is changed from  $27000 \text{ W/m}^2\text{K}$  to  $77000 \text{ W/m}^2\text{K}$  which is approximately 3 times higher than 1 L/min simulation. It is not only applicable to impingement zone but also the differences are significant on other locations as well. This implies that the cooling flow rate has great impact on HTC values.

Velocity contour from converged solution for the flow rate of 1 L/min is shown in Figure 10. The velocity is increased locally after the impingement zone because of the presence of large separation vortex near the sharp turn. This flow separation is created due to 180 deg bend in the flow. From Figure 8, it is observed that the maximum HTC value is recorded where the velocity reaches local maxima after the stagnation point.

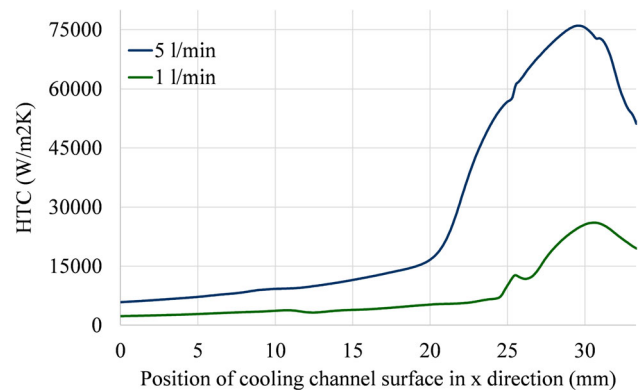


Fig. 9—HTC plots on the cooling channel surface for different flow rates.

To validate the coupled modeling approach, a case study was conducted where the actual porosity disappeared upon introduction of cooling in the core pin. Casting simulations for 3 different cases were performed as shown in Figure 11. The location where a casting defect is expected is designated as a “Hot Spot” in the die casting literature. The results indicates that by revising the HTC values, the “Hot Spot” near the core pin is disappeared—this is in agreement with the experiments. This is due to the higher values of HTC that are evidently closer to reality as derived from the coupled modeling approach. Also, the fraction of liquid at the end of solidification was monitored for these cases. It is noted that 7 pct of isolated liquid at the solidification time of 12 sec is disappeared in the simulation performed with the calculated HTC values.

### III. EXPERIMENTAL VALIDATION

#### A. Experimental Setup

A K-type thermocouple of 0.5 mm probe size was mounted in the core pin without interfering with the cooling adaptors (Figure 12). Copper paste was applied in front of the thermocouple to avoid the air gap between the surface and thermocouple.<sup>[15]</sup> Also, a stopper plate was provided at the back side of the thermocouple to ensure that the tip was always in contact with the die surface as shown in Figure 12. Flow meters were connected at inlet and outlet of the cooling channel. The flow meters and the thermocouple were interfaced with a data logging device to monitor and automatically record the flow rates and temperatures over a period of time. AlSi10MgMn alloy was used for conducting the experiment. To study the influence of flow rate, investigations were conducted at two different flow rates *i.e.*, 1 L/min and 5 L/min, respectively.

#### B. Die Temperature Comparison for Different Flow Rates

Figure 13 shows temperature readings (die temperature and cooling water temperature difference) for one complete cycle of die casting process with cooling water flow rates of 1 and 5 L/min. The HPDC process is

divided into 5 major stages *i.e.*, injection, solidification, die opening and extraction, die spraying and air blowing and die closing and ladling.<sup>[16]</sup> The complex stage in HPDC is during the phase transformation in the molten alloy because of rapid solidification. The focus of this study is on the solidification stage and hence the HTC of cooling channel is critically important. Figure 13 shows that the die temperatures at 5 L/min flow rate has lower values than that with 1 L/min flow rate.

#### C. Comparison of Thermal Image, CT Scan and Microscopic Images

Thermographic images of core pin were taken using infrared camera after solidification and images for 1 and 5 L/min flow rates were compared (Figure 14). Twenty points were randomly picked in the core pin and the temperature values corresponding to these points are plotted in Figure 15. A temperature difference of 20 °C and 10 °C are observed between the two flow rates in circumferential zone and impinging zone of core pins, respectively. In addition, it is noticed that temperature of the core pin at the tip zone is lower than the circumferential zone. This is due to the fact that HTC values near the tip zone are higher than the circumferential zone as shown in Figure 8.

Castings produced for both the coolant flow rates were inspected through computed tomography scan machine (CT scan).<sup>[17,18]</sup> Because of the higher solidification rate with 5 L/min flow rate, the intensity of porosity is reduced significantly compared to 1 L/min flow rate (Figure 16). Eight out of 20 castings produced were taken for both the flow rates and their porosity volumes are plotted in Figure 17. An average porosity volume difference of 125 mm<sup>3</sup> is observed between the two flow rates in agreement with the literature. As shown in Figure 18, the faster solidification rates results in finer dendrites with 5 L/min flow rate whereas coarse dendrites are noticed in castings with 1 L/min flow rate.<sup>[19,20]</sup>

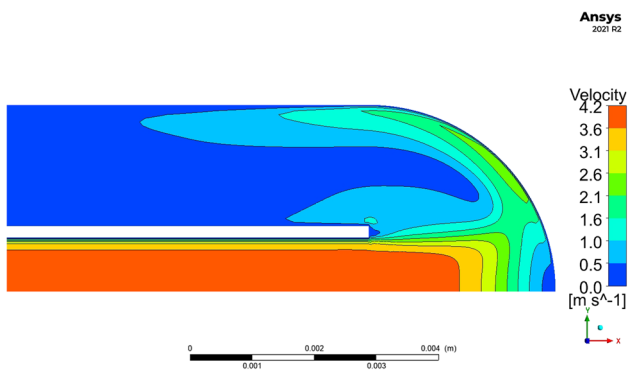


Fig. 10—Velocity contours of water flow field for  $V = 4.2$  m/s.

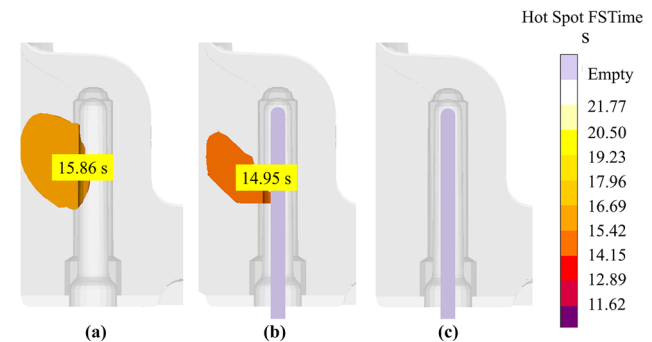


Fig. 11—Casting simulation comparison—Hot Spot results. (a) Without cooling (b) with cooling (average HTC values) (c) with cooling (calculated HTC values).

#### D. Comparison of Simulation with Actual Die Temperature

Figure 19 shows the comparison of the calculated die temperature from the coupled modeling approach with the experiment. There is a good agreement observed between the simulation and the experiment. A maximum of 14 °C difference is observed between these two curves. This is acceptable in die casting because of inherent process variability and numerical errors in the simulation. Also the experimental readings are closer to the simulation for 5 L/min flow rate. Hence, the modified HTC values using coupled modeling approach are accurate enough to predict the actual behaviour of castings.

### IV. PARAMETRIC STUDY

#### A. Factors and Levels

Parametric study was carried out to understand the effect of different design parameters in cooling channel and velocity of cooling water in the channel on the heat removal rate. Through careful examination, important

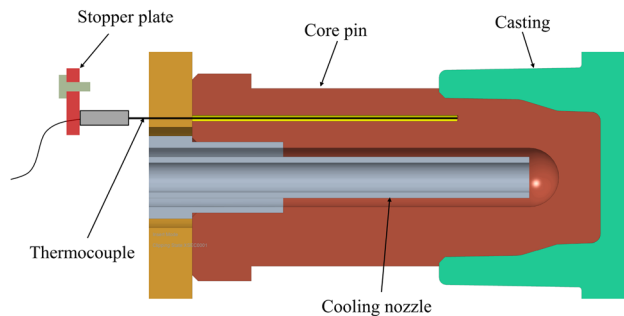


Fig. 12—Thermocouple instrumentation in die.

parameters that have most influence on response were selected and levels were identified. These parameters were: (1) cooling hole diameter ( $D$ ), (2) nozzle diameter ( $d$ ), (3) nozzle to die surface gap ( $h$ ) and (4) inlet velocity of water ( $V$ ). The values used in current practice were taken as base level. Upper and lower levels were fixed on the basis as stated below.

- Cooling hole diameter cannot exceed 12 mm because of less wall thickness in core pin and cannot be decreased below 8 mm because of standard thread size.
- Levels of nozzle diameter were taken in such a way that outlet area should be greater than inlet area as per industrial practice.
- Considering the variations in manufacturing and assembly, the upper and lower levels of Nozzle-to-die surface gap were allotted as 1 mm above and 1 mm below the current levels respectively.
- Based on the capacity of the pump in the die casting machine used for the experiments, the levels of velocities were decided.

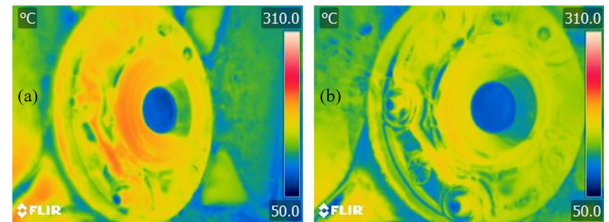


Fig. 14—Thermal images of die using infrared camera. (a) 1 L/min (b) 5 L/min.

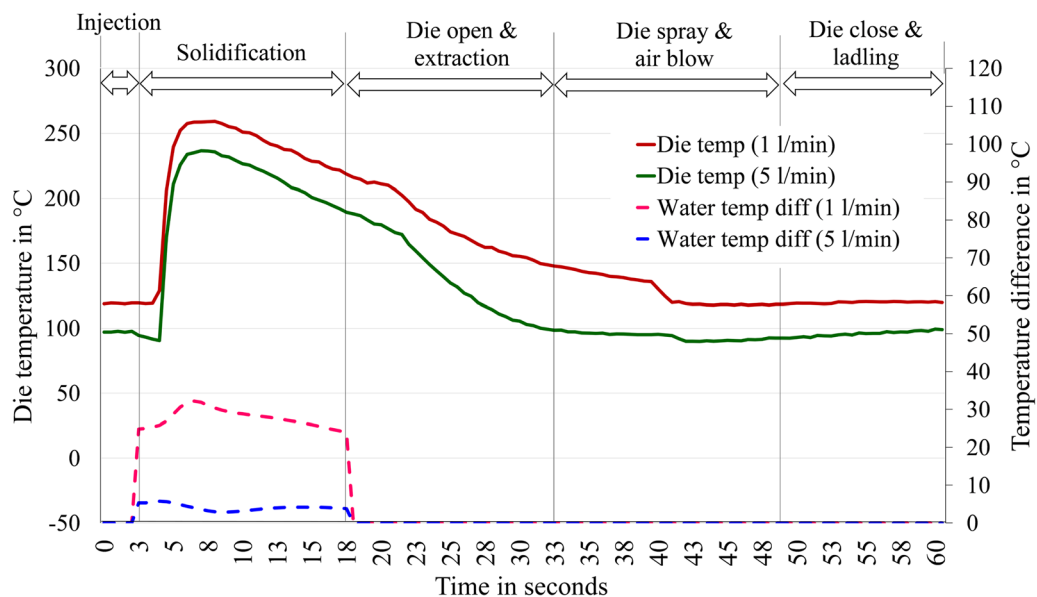


Fig. 13—Variation of die temperature (left vertical axis) and temperature difference between outlet and inlet (right vertical axis) with time for complete die casting cycle.

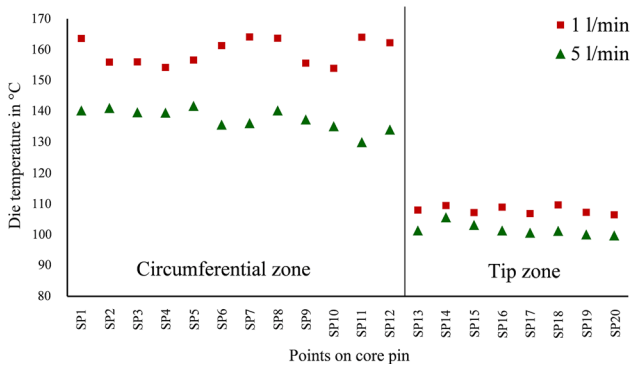
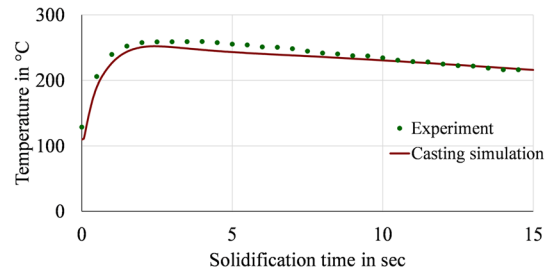
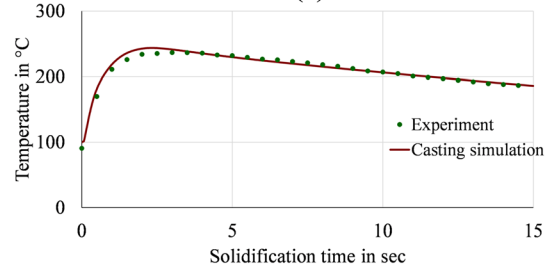


Fig. 15—Die temperature comparison from thermal images. SP1-SP12 are taken on circumference of core pin and SP13-SP20 are taken on flat face of core pin.



(a)



(b)

Fig. 19—Die temperature comparison between simulation and experiment. (a) 1 L/min, (b) 5 L/min.

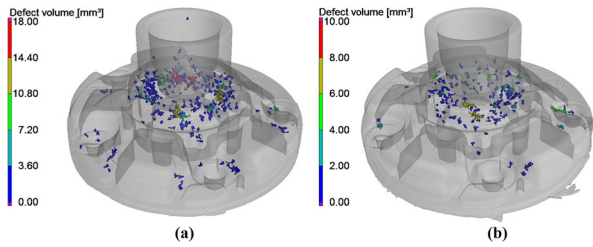


Fig. 16—Porosity volume comparison through CT scan. (a) 1 L/min, (b) 5 L/min.

Table II. Parametric Study—List of Factors and Their Values

$D$ (mm)	8	10	12
$d$ (mm)	3	4	5
$h$ (mm)	3	4	5
$V$ (m/s)	3	4	5

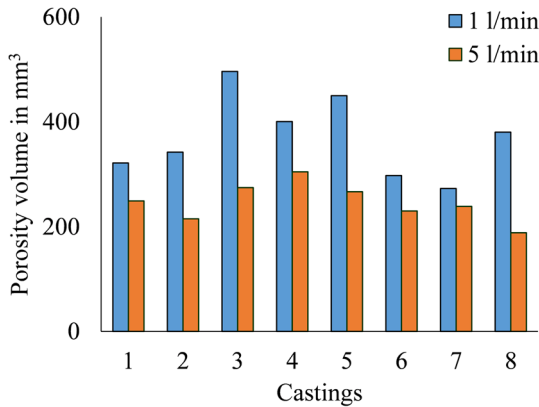


Fig. 17—Porosity volume comparison for 1 and 5 L/min flow rates.

The list of factors and their values selected for the parameter study are listed in Table II. Since the lower level of nozzle diameter for cooling hole diameter of 12 mm violated the area ratio, that level was ignored for study. Each combination of a factor and a level is said to be a design point. Combining all factors and levels, there were totally 72 design points possible (full factorial condition).

### B. Results from the Parametric Study

All the design points were simulated numerically using the cooling channel simulation. The heat removed by water from the core pin was taken as the output response. The values of heat removal rate (J/s) are plotted against design points in Figure 20.

To show the effect of individual factor and level, they are differentiated with marker shape, color and border line width. It can be clearly observed that increase in velocity always results in increase of heat removal rate. The same is also true for nozzle diameter except when the cooling hole diameter is kept as 12 mm. Similarly, when the cooling hole diameter is increased from level 1 to level 2, the average values of heat removal rate is increased significantly whereas the values are not significant for the change between level 2 and level 3. This can be easily understood through main effects plot

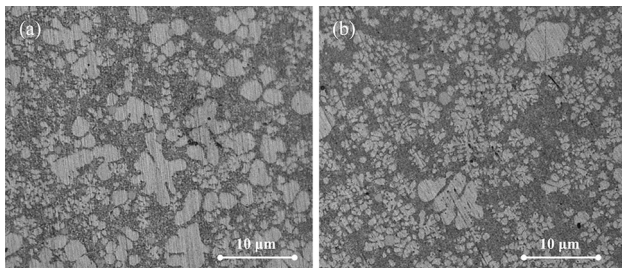


Fig. 18—Micro-structure/dendrites comparison. (a) 1 L/min, (b) 5 L/min.



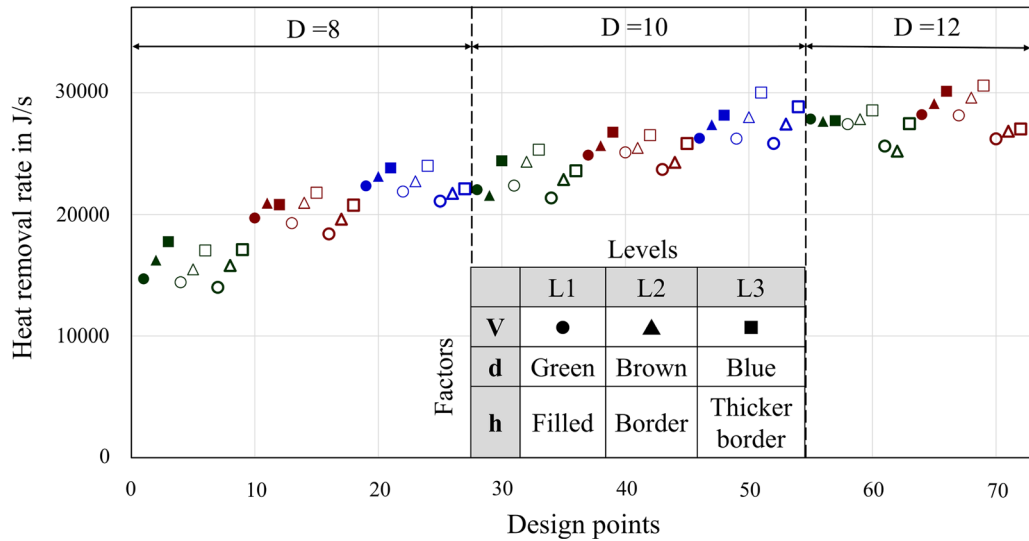


Fig. 20—Plot of heat removal rate with design points.

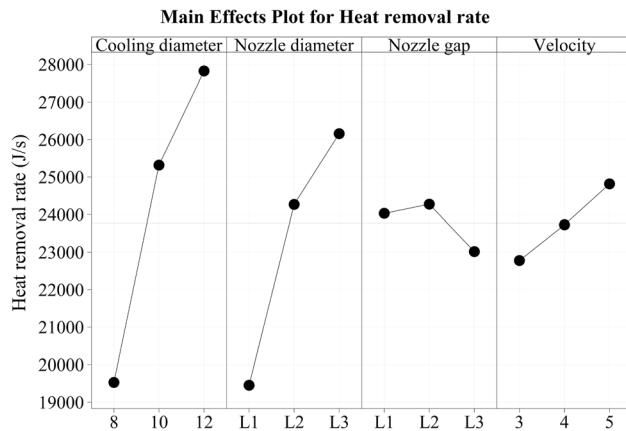


Fig. 21—Main effect plot—heat removal rate.

(Figure 21). The most influencing factors in the decreasing order are cooling hole diameter, nozzle diameter and velocity of inlet water. The role of nozzle-to-die surface gap is insignificant on heat removal rate.

## V. CONCLUSION

This study considered the effect of turbulent flow in the cooling channel on the heat transfer characteristics in a typical HPDC process through numerical and experimental investigations. The following conclusions are drawn:

1. Coupled modeling approach was developed ensuring accurate heat transfer coefficient in the cooling channel. There is a remarkable gap observed between the recommended HTC value and the calculated value from coupled modeling approach. The maximum

HTC value of  $7000 \text{ W/m}^2\text{K}$  is recommended near the impingement zone in casting simulation whereas the calculated HTC function reaches the peak value of  $27,000 \text{ W/m}^2\text{K}$ .

2. A casting simulation is performed using the revised HTC values and the same is validated by conducting experiment in actual die casting machine. The die temperature from the casting simulation using the coupled approach is seen to closely match with the measurements.
3. The influence of flow rate on HTC was also investigated numerically and experimentally. Numerical results implies that there is a significant increase in HTC values between the coolant flow rates of 1 and 5 L/min. The maximum HTC value changed from  $27,000$  to  $77,000 \text{ W/m}^2\text{K}$ . This increase in HTC values was also evidenced in experimental results such as thermal imaging of die, casting porosity volumes and microstructures.
4. The false positive (hot spot) in the prediction from the casting simulation was corrected by revising the HTC values. With the calculated HTC values, the hot spot is eliminated. Similarly intensity of porosity is reduced significantly and moved away from the core pin.
5. Parametric studies were performed numerically using cooling channel simulation by changing cooling hole diameter, nozzle diameter, nozzle to die surface gap and inlet velocity of water. The maximum heat removal is obtained when the cooling hole diameter, nozzle diameter and velocity of water are in the upper level. There is no significant change on heat removal rate with change of nozzle-to-surface gap.

## CONFLICT OF INTEREST

On behalf of all authors, the corresponding author states that there is no conflict of interest.

## REFERENCES

1. M. Khan and A. Sheikh: *Int. J. Simul. Model.*, 2018, vol. 17(2), pp. 197–209. <https://doi.org/10.1016/j.ijheatmasstransfer.2010.09.021>.
2. J. Fu: PhD thesis, Purdue University, 2016. [https://docs.lib.purdue.edu/open\\_access\\_theses/849](https://docs.lib.purdue.edu/open_access_theses/849).
3. M. Karkkainen and L. Nastac: *JOM*, 2019, vol. 71(2), pp. 772–78. <https://doi.org/10.1007/s11837-018-3261-x>.
4. F. Sun and G.-X. Wang: in: *ASME International Mechanical Engineering Congress and Exposition*, vol. 43025, pp. 895–901, 2007. <https://doi.org/10.1115/IMECE2007-42520>.
5. L. Chen, Y.-L. He, Q. Kang, and W.-Q. Tao: *J. Comput. Phys.*, 2013, vol. 255, pp. 83–105. <https://doi.org/10.1016/j.jcp.2013.07.034>.
6. Y.-T. Yang, T.-C. Wei, and Y.-H. Wang: *Int. J. Heat Mass Transf.*, 2011, vol. 54(1–3), pp. 482–89. <https://doi.org/10.1016/j.ijheatmasstransfer.2010.09.021>.
7. N. Souris, H. Liakos, and M. Founti: *AIChE J.*, 2004, vol. 50(8), pp. 1672–83. <https://doi.org/10.1002/aic.10171>.
8. E. Öztekin, O. Aydin, and M. Avci: *Int. Commun. Heat Mass Transf.*, 2013, vol. 44, pp. 77–82. <https://doi.org/10.1016/j.icheatmasstransfer.2013.03.006>.
9. M. Sharif and K. Mothe: *Int. J. Therm. Sci.*, 2010, vol. 49(2), pp. 428–42. <https://doi.org/10.1016/j.ijthermalsci.2009.07.017>.
10. J. Taghinia, M.M. Rahman, and T. Siikonen: *Chin. J. Chem. Eng.*, 2016, vol. 24(5), pp. 588–96. <https://doi.org/10.1016/j.cjche.2015.12.009>.
11. M. Sharif and K. Mothe: *Numer. Heat Transf. Part B Fundam.*, 2009, vol. 55(4), pp. 273–94. <https://doi.org/10.1080/10407790902724602>.
12. I. Fluent: *Fluent 14.5 User Guide*. NH-03766, Fluent Inc., Lebanon, 2002.
13. MAGMA: *MAGMASOFT User Manual*, MAGMA GmbH Kackertstrasse, Aachen, Germany, 1996.
14. M. Navarro Aranda: Master's thesis, Jönköping University, 2015. <http://urn:nbn:se:hj:diva-28023>.
15. G. Zhi-peng, X. Shou-mei, L. Bai-cheng, M. Li, and J. Allison: *Int. J. Heat Mass Transf.*, 2008, vol. 51(25–26), pp. 6032–38. <https://doi.org/10.1016/j.ijheatmasstransfer.2008.04.029>.
16. F. Bonollo, N. Gramegna, and G. Timelli: *JOM*, 2015, vol. 67(5), pp. 901–08. <https://doi.org/10.1007/s11837-015-1333-8>.
17. Y. Zhang, J. Zheng, Y. Xia, H. Shou, W. Tan, W. Han, and Q. Liu: *Mater. Sci. Eng. A*, 2020, vol. 772, p. 138781. <https://doi.org/10.1016/j.msea.2019.138781>.
18. F.A. Al Mufadi and M.A. Irfan: *Mater. Tes.*, 2015, vol. 57(5), pp. 398–401. <https://doi.org/10.3139/120.110727>.
19. D.M. Stefanescu: *Science and Engineering of Casting Solidification*, Springer, Cham, 2015.
20. K.O. Yu: *Modeling for Casting and Solidification Processing*, CRC Press, Boca Raton, 2001.

**Publisher's Note** Springer Nature remains neutral with regard to jurisdictional claims in published maps and institutional affiliations.

Springer Nature or its licensor (e.g. a society or other partner) holds exclusive rights to this article under a publishing agreement with the author(s) or other rightsholder(s); author self-archiving of the accepted manuscript version of this article is solely governed by the terms of such publishing agreement and applicable law.